Ferroelectric Transitions at Ferroelectric Domain Walls Found from First Principles

Jacek C. Wojdeł and Jorge Íñiguez
Institut de Ciència de Materials de Barcelona (ICMAB-CSIC), Campus UAB, 08193 Bellaterra, Spain
(Received 25 February 2014; published 20 June 2014)

We present a first-principles study of model domain walls (DWs) in prototypic ferroelectric $PbTiO_3$. At high temperature the DW structure is somewhat trivial, with atoms occupying high-symmetry positions. However, upon cooling the DW undergoes a symmetry-breaking transition characterized by a giant dielectric anomaly and the onset of a large and switchable polarization. Our results thus corroborate previous arguments for the occurrence of ferroic orders at structural DWs, providing a detailed atomistic picture of a temperature-driven DW-confined transformation. Beyond its relevance to the field of ferroelectrics, our results highlight the interest of these DWs in the broader areas of low-dimensional physics and phase transitions in strongly fluctuating systems.

DOI: 10.1103/PhysRevLett.112.247603 PACS numbers: 77.80.B-, 63.70.+h, 71.15.Mb

The structural domain walls (DWs) occurring in ferroelectric (FE) and ferroelastic (FS) materials have become a focus of attention. Recent studies show that the DWs can present a variety of properties, from conductive [1–4] and optical [5,6] to magnetic [7–9], that differ from those of the neighboring domains, which suggests that they could be the active element in nanotechnological applications [10,11]. Elucidating the DW behavior poses major experimental challenges, and the origin of most of the newly discovered effects remains unclear. In fact, we still lack a detailed structural and dynamical picture of the DWs, and in many cases we can only speculate about the structure–property relationships at work within them. Hence, there is a pressing need for predictive theoretical studies tackling the DWs at an atomistic level and at the relevant conditions of temperature, etc.

The DW structure, and even the possible occurrence of DW-confined ferroic orders, have been discussed theoretically for decades, usually in the framework of continuum Ginzburg-Landau or phenomenological model theories [12–22]. Materials with competing structural instabilities have been a focus of attention, a good example being perovskite $SrTiO_3$ (STO). STO undergoes a FS transition driven by an antiferrodistortive (AFD) mode that involves concerted rotations of the O_6 octahedra in the perovskite structure. This mode competes with a FE instability that is suppressed by the onset of the AFD distortion [23]. Yet, there are both theoretical and experimental indications that a polar order occurs at low temperatures *within STO's FS DWs* [16,24–26], i.e., in the region where the otherwise dominant AFD distortions vanish. In this context, it is worth noting recent first-principles studies predicting that $PbTiO_3$ (PTO) [27] and related compounds [28] present a FE-AFD competition that is even stronger than the one occurring in STO. These are the ideal conditions to obtain interesting effects at structural DWs, and motivated this work.

Low-temperature study.—We employed the tools of Ref. [27], which permit large-scale simulations with first-principles predictive power, to investigate an ideal version of the simplest DWs occurring in PTO, namely, 180° boundaries separating regions of opposed polarization and being perfectly planar. We used the model potential for PTO labeled "L^I" [27], which we briefly describe in [29]. As shown in Fig. 1(a), we set the polarization of the first domain $\mathbf{P}^{\mathrm{I}}$ parallel to the [100] direction of the perovskite lattice, and took $\mathbf{P}^{\mathrm{II}} \| [\bar{1}00]$ for the second one; the DW in between was assumed to reside in a (001) plane. Our supercell, which contains $12 \times 12 \times 20$ perovskite units (14400 atoms), is periodically repeated and holds two DWs.

We investigated the ground state structure of this multidomain configuration by means of Monte Carlo (MC) simulated annealings [29]. Figure 1(b) shows the x component of the polarization (P_x) as we move along z. We observe two domains within which PTO adopts the structure of its homogeneous ground state, with an associated polarization of about 0.99 $\mathrm{C/m^2}$ and a cell aspect ratio of about 1.07. The domains are separated by a DW centered at a PbO plane and presenting a thickness of about one unit cell.

Our DWs do not display any rotations of the O_6 octahedra. This result lends itself to a simple explanation: Because the DWs are ultrathin, hypothetical DW-localized AFD modes would *overlap* with the neighboring FE distortions and thus be penalized by the FE-AFD competition. As a result, the absence of localized AFD modes seems rather natural.

Nevertheless, the structure of the DWs is far from being trivial. As shown in Fig. 1(c), a nonzero P_y polarization appears at the DW plane and rapidly vanishes as we move into the domains. This DW polarization is switchable, as evidenced by the hysteresis loop in Fig. 2(a). Further calculations show that the polarizations of neighboring

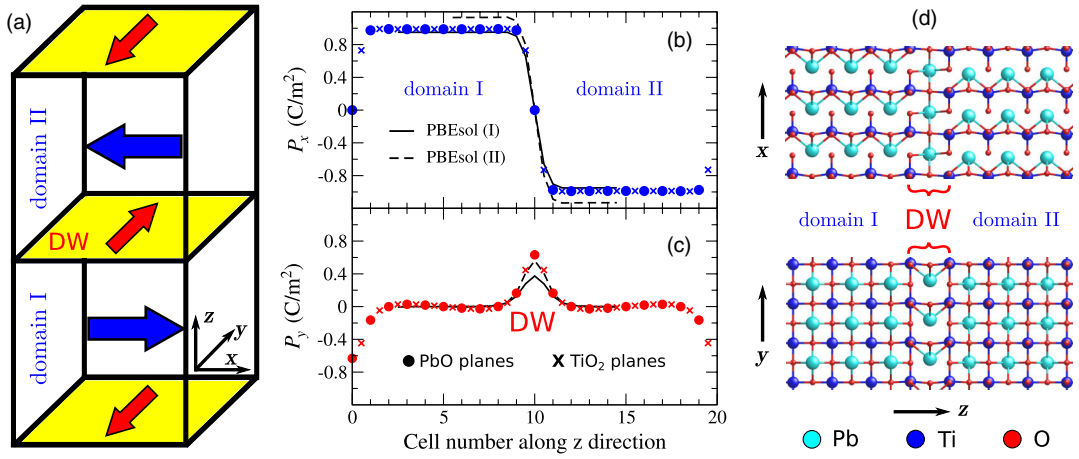

FIG. 1 (color online). Panel (a): Sketch of the supercell used in our simulations. The indicated Cartesian axes coincide with the principal directions of the perovskite lattice. Panels (b) and (c): Polarization profile corresponding to the stable structure of our multidomain configuration. (Calculation of local polarizations described in Ref. [29].) The "PBEsol (I)" lines show the results of an unconstrained first-principles structural relaxation [29]; the agreement with the model predictions is essentially perfect for the P_x profile; for the DW polarization we obtain a slightly smaller value. The "PBEsol (II)" lines show the results of a first-principles relaxation in which the supercell lattice parameters were fixed to match those predicted by our model potential; the agreement for the P_y profile is essentially perfect; for the polarization within the domains we get slightly larger values. Panel (d): Views of the atomic structure of our multidomain configuration.

DWs couple, and tend to align in a parallel configuration when the walls are sufficiently close. However, the DW–DW interaction quickly decreases with the separation distance; for example, for our $12 \times 12 \times 20$ supercell, the energy split between the parallel and antiparallel states is about 0.01 meV per DW cell, which is negligible. Hence, the antiparallel configuration shown in Fig. 1 is a stable state (i.e., a local minimum of the energy), but not more significant than the also stable, quasidegenerate parallel configuration.

Our results show how strain and the reduced dimensionality determine the energetics of the DW-confined FE distortion. The onset of the multidomain structure for P_x implies a strong deformation of the perovskite lattice: it becomes tetragonal and acquires an aspect ratio of 1.07, the long lattice vector coinciding with the polar axis x. In the case of our simulated system, the xy plane is homogeneously strained throughout the supercell (stretched along x, shrunk along y). Hence, even if we have $P_x = 0$ at the DWs of Fig. 1, the strain disfavors the occurrence of a DW polarization along the y direction, which is subject to a compression. The ensuing effect can be appreciated in the potential wells of Fig. 2(b): Case I corresponds to the full development of the FE distortion of PTO, as it happens within the domains. Case II corresponds to the development of a three-dimensional y-polarized state when we constrain the cell to be strained as in the x-polarized FE state; the equilibrium polarization and associated energy gain get clearly reduced, and we obtain a value of P_y (about 0.75 C/m^2) that is not far from our result at the DW center (about 0.65 C/m^2). Additionally, Fig. 2(b) shows a case III corresponding to the condensation of P_y at our DWs; the energy well becomes shallower than in case II, indicating a further weakening of the polar instability caused by the spatial confinement (i.e., by the truncation of interactions favoring the three-dimensional homogeneous polar state) and the competition with the P_x distortion of the neighboring domains. Nevertheless, the obtained well depth (86 meV/cell) is sizable, which suggests that the predicted DW instability should occur at relatively high temperatures.

We checked the correctness of our model-potential predictions by running direct first-principles calculations of our multidomain structure, using a $1 \times 1 \times 20$ cell. As shown in Figs. 1(b) and 1(c), the agreement between our model-potential and first-principles results is very good, and the FE character of PTO's DWs is confirmed [30]. We should note that there are several first-principles studies of the 180° DWs of PTO in the literature [18,31–33], and the consensus is that no DW-confined polarization occurs. We cannot be sure about the reasons why these previous works did not find polarized DWs; some possibilities are discussed in [29].

We checked whether this confined polarization occurs in other PTO DWs. We found that 180° DWs lying in other planes—e.g., a (011) boundary separating domains with $\mathbf{P}^{\mathrm{I}} \| [100]$ and $\mathbf{P}^{\mathrm{II}} \| [\bar{1}00]$—present polar distortions analogous to the one just described. In contrast, we found that 90° DWs do not present any FE instability, a result probably related with the fact that these boundaries are considerably more distorted than their 180° counterparts, or to the elastic (epitaxial tensile) constraints we had to impose in order to stabilize them. PTO's 90° DWs will be discussed elsewhere.

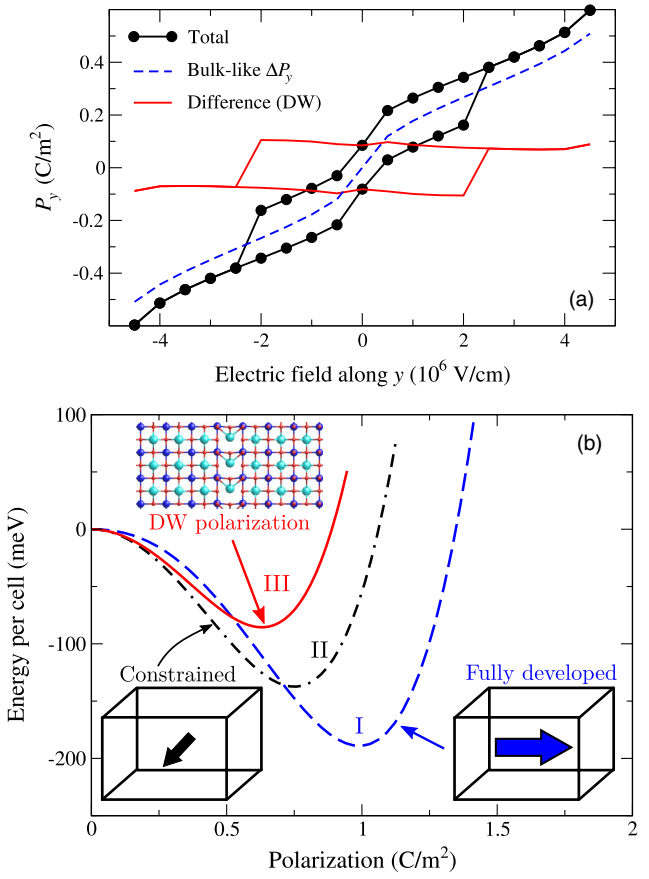

FIG. 2 (color online). Panel (a): Polarization loop computed for the x-polarized multidomain state of Fig. 1 and for an electric field along the y direction. For these simulations we used a $1 \times 1 \times 20$ supercell, thus assuming an homogeneous switch, and performed the calculations in the limit of 0 K (details in [29]). The total response (black line and circles) is split in two parts: (1) The response of an x-polarized monodomain state (dashed blue line); note that this response does not saturate, as the P_x polarization will eventually rotate to align with the field. (2) The difference between the total and the monodomain results (solid red line), which captures the DW response. In order to observe the switch at the DWs, we imposed in the simulations the strain of the multidomain ground state, and thus prevented the domain polarizations from fully aligning with the applied field for relatively small field values. Such a constraint is similar to the epitaxial one characteristic of thin films. Panel (b): Energy wells corresponding to FE instabilities in various situations described in the text. Note that the $P = 0$ state corresponds to a different atomistic configuration in each case. In the case of the DW polarization (red solid line) the energy is given *per* cell within the DW plane.

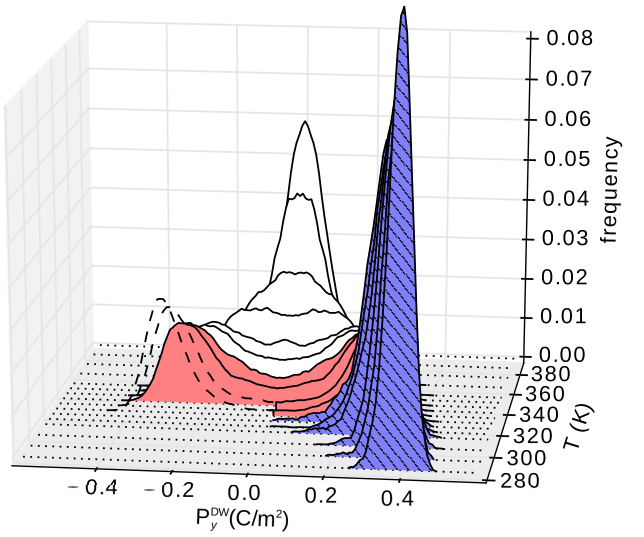

FIG. 3 (color online). Probability distribution $\rho(P_y^{\mathrm{DW}})$ for the y component of the polarization at the center of the DW and as a function of temperature. The three temperature regions mentioned in the text are marked with different colors: white for $T \geq 350$ K (where we clearly have $\langle P_y^{\mathrm{DW}} \rangle = 0$), red for 320 K $< T <$ 350 K (critical region), and blue with stripes for $T \leq 320$ K (where we clearly have $\langle P_y^{\mathrm{DW}} \rangle \neq 0$). The left side of the histograms for $T = 330$ K and $T = 325$ K is drawn using dashed black lines; this is to emphasize that, at these temperatures, we attribute the P_y^{DW} fluctuations from positive to negative values to finite size effects (see [29]).

Finally, let us note that the low-temperature configuration of our PTO DWs can be described as being Bloch-like. First-principles theory has predicted the occurence of Bloch-like DW configurations in materials like $LiNbO_3$ [18] and $BaTiO_3$ in its rhombohedral phase [21].

Behavior with temperature.—We studied PTO DWs as a function of increasing temperature by running MC simulations as described in [29]. Figure 3 shows the obtained probability density, $\rho(P_y^{\mathrm{DW}})$, for the y component of the polarization at the DW plane. We observe three distinct regions. (1) For $T \leq 320$ K the DW presents a stable and large polarization, and the equilibrium state resembles the one discussed above. (2) For $T \geq 350$ K the DW gets disordered and we have a null thermal average $\langle P_y^{\mathrm{DW}} \rangle = 0$. At those temperatures the system presents a mirror symmetry plane perpendicular to the y axis, and we could say that the DWs are in a *paraelectric* state [34]. (3) Finally for 320 K $< T <$ 350 K we have a narrow region in which, during the course of the MC simulation, P_y^{DW} occasionally switches between equivalent polar states. Clearly, the finite size of our simulation supercell is partly responsible for such fluctuations, which should be considered a spurious finite size effect below a certain transition temperature T_C^{DW}. At any rate, the presence of a phase transition is obvious from these results, and the analysis of the MC data suggests that we have $T_C^{\mathrm{DW}} \approx 335$ K. (See [29] for details.)

The phase transitions in our simulated system are clearly appreciated in Fig. 4, which shows the evolution of the relevant order parameters and dielectric response. As the system cools down from high T, the diagonal components of the dielectric tensor increase sharply, revealing a FE transition at $T_C = 510$ K. (The quantitative disagreement between our computed T_C and the experimental result for PTO (760 K) is discussed in Ref. [27].) Note that for

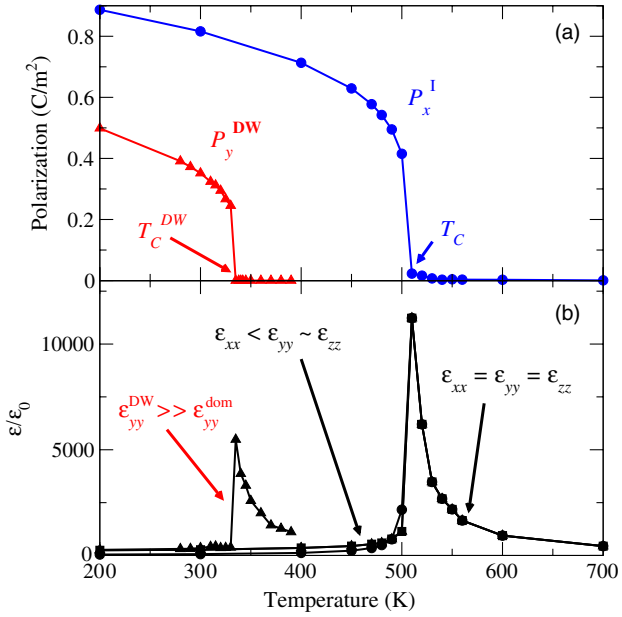

FIG. 4 (color online). Panel (a): Temperature dependent polarization at the center of the first domain (P_x^{I}, blue circles) and at the center of the DWs (P_y^{DW}, red triangles). Panel (b): Diagonal components of the dielectric permittivity tensor. The discontinuity for ϵ_{yy} (triangles) at $T = 390$ K is related with the finite-size effects described in [29].

$T > 510$ K we have $\epsilon_{xx} = \epsilon_{yy} = \epsilon_{zz}$, reflecting the cubic symmetry of the paraelectric phase. Then, for $T \gtrsim T_C^{DW}$ the ϵ_{yy} component [triangles in Fig. 4(b)] behaves in an anomalous way. As regards the dielectric response along the y direction, our multidomain configuration can be viewed as a set of parallel capacitors, so that the total dielectric constant can be split into domain and DW contributions, $\epsilon_{yy} = f^{\mathrm{dom}}\epsilon_{yy}^{\mathrm{dom}} + f^{\mathrm{DW}}\epsilon_{yy}^{\mathrm{DW}}$, where f^{dom} and f^{DW} are the respective volume fractions. Noting that $f^{\mathrm{dom}} \approx 0.9$ and $f^{\mathrm{DW}} \approx 0.1$ in our case, and that $\epsilon_{yy}^{\mathrm{dom}}$ is featureless for $T < T_C$ (which we checked by running MC simulations of the monodomain case), it is clear that the increase in ϵ_{yy} comes from a very large DW response $\epsilon_{yy}^{\mathrm{DW}}$. Hence, the DW-confined transition is driven by a FE soft mode and characterized by very strong fluctuations of the order parameter, as consistent with the reduced dimensionality.

Final remarks.—As mentioned, the possibility of having polar orders and dielectric anomalies associated with DWs has been discussed in the theoretical literature, typically employing phenomenological continuum models [16,22]. Our first-principles work corroborates that such effects can indeed occur, providing for the first time a realistic atomistic picture of a T-driven DW-confined ferroic transformation.

One might describe the found transition as a change in the DW character, from Bloch to Ising, upon heating; in fact, some authors have discussed similar effects in these terms [20,22]. However, we think that our result is better described as a proper FE phase transition confined to the DW, to emphasize that it results in a switchable DW polarization. For the same reasons, we would rather denote the low-temperature state as a ferroelectric DW, and not simply as a DW with Bloch-like character. Note that, as in the case of $LiNbO_3$ [18], Bloch-like DWs may not display a net polarization.

The present results are the first step in the investigation of such an interesting phenomenon. Aspects for future work include: the possible critical behavior of the transition, the pre-transitional dynamics, the internal structure of the DWs (can we have multidomain states within them?), and the role of DW–DW interactions (can it affect the dimensionality and features of the transition?). We thus believe our findings will open exciting research avenues in the fields of phase transitions and low-dimensional physics.

It may seem surprising that the predicted effect has not been reported experimentally. However, note that observing such an FE order may require some uncommon measurements. Ideally, one would like to work with samples presenting a pattern of highly ordered stripe domains separated by 180° DWs, as displayed by suitably grown PTO films [35] and PTO/STO superlattices [36,37]. High-resolution x-ray measurements at low temperatures may reveal the DW order. Additionally, by measuring the dielectric response along the in-plane direction of the DWs, one should be able to observe a clear feature around T_C^{DW}. We hope our results will motivate further experimental work to characterize FE DWs and the transitions that may occur within them.

Work supported by MINECO-Spain (Grants No. MAT2010-18113 and No. CSD2007-00041) and CSIC [JAE-doc program (JCW)]. Some figures were prepared using VESTA [38]. We thank Ekhard Salje, David Vanderbilt, and Pavlo Zubko for their useful comments.

[1] J. Seidel, L. W. Martin, Q. He, Q. Zhan, Y. H. Chu, A. Rother, M. E. Hawkridge, P. Maksymovych, P. Yu, M. Gajek, N. Balke, S. V. Kalinin, S. Gemming, F. Wang, G. Catalan, J. F. Scott, N. A. Spaldin, J. Orenstein, and R. Ramesh, Nat. Mater. **8**, 229 (2009).
[2] J. Guyonnet, I. Gaponenko, S. Gariglio, and P. Paruch, Adv. Mater. **23**, 5377 (2011).
[3] S. Farokhipoor and B. Noheda, Phys. Rev. Lett. **107**, 127601 (2011).
[4] A. Aird and E. K. H. Salje, J. Phys. Condens. Matter **10**, L377 (1998).
[5] S. Y. Yang, J. Seidel, S. J. Byrnes, P. Shafer, C. H. Yang, M. D. Rossell, P. Yu, Y. H. Chu, J. F. Scott, J. W. Ager, L. W. Martin, and R. Ramesh, Nat. Nanotechnol. **5**, 143 (2010).
[6] M. Alexe and D. Hesse, Nat. Commun. **2**, 256 (2011).

[7] Q. He, C. H. Yeh, J. C. Yang, G. Singh-Bhalla, C. W. Liang, P. W. Chiu, G. Catalan, L. W. Martin, Y. H. Chu, J. F. Scott, and R. Ramesh, Phys. Rev. Lett. **108**, 067203 (2012).
[8] M. Daraktchiev, G. Catalan, and J. F. Scott, Phys. Rev. B **81**, 224118 (2010).
[9] Z. V. Gareeva and A. K. Zvezdin, Phys. Solid State **52**, 1714 (2010).
[10] E. K. H. Salje, ChemPhysChem **11**, 940 (2010).
[11] G. Catalan, J. Seidel, R. Ramesh, and J. F. Scott, Rev. Mod. Phys. **84**, 119 (2012).
[12] B. Strukov and A. Levanyuk, *Ferroelectric Phenomena in Crystals: Physical Foundations* (Springer, New York, 1998).
[13] A. Tagantsev, L. E. Cross, and J. Fousek, *Domains in Ferroic Crystals and Thin Films* (Springer, New York, 2010).
[14] J. J. Lajzerowicz and J. J. Niez, J. Phys. Lett. **40**, 165 (1979).
[15] B. Houchmandzadeh, J. Lajzerowicz, and E. Salje, J. Phys. Condens. Matter **3**, 5163 (1991).
[16] A. K. Tagantsev, E. Courtens, and L. Arzel, Phys. Rev. B **64**, 224107 (2001).
[17] L. Goncalves-Ferreira, S. A. T. Redfern, E. Artacho, and E. K. H. Salje, Phys. Rev. Lett. **101**, 097602 (2008).
[18] D. Lee, R. K. Behera, P. Wu, H. Xu, Y. L. Li, S. B. Sinnott, S. R. Phillpot, L. Q. Chen, and V. Gopalan, Phys. Rev. B **80**, 060102 (2009).
[19] S. Conti, S. Müller, A. Poliakovsky, and E. K. H. Salje, J. Phys. Condens. Matter **23**, 142203 (2011).
[20] V. Stepkova, P. Marton, and J. Hlinka, J. Phys. Condens. Matter **24**, 212201 (2012).
[21] M. Taherinejad, D. Vanderbilt, P. Marton, V. Stepkova, and J. Hlinka, Phys. Rev. B **86**, 155138 (2012).
[22] P. Marton, V. Stepkova, and J. Hlinka, Phase Transit. **86**, 103 (2013).
[23] W. Zhong and D. Vanderbilt, Phys. Rev. Lett. **74**, 2587 (1995).
[24] J. F. Scott, E. K. H. Salje, and M. A. Carpenter, Phys. Rev. Lett. **109**, 187601 (2012).
[25] E. A. Eliseev, A. N. Morozovska, Y. Gu, A. Y. Borisevich, L.-Q. Chen, V. Gopalan, and S. V. Kalinin, Phys. Rev. B **86**, 085416 (2012).
[26] E. K. H. Salje, O. Aktas, M. A. Carpenter, V. V. Laguta, and J. F. Scott, Phys. Rev. Lett. **111**, 247603 (2013).
[27] J. C. Wojdeł, P. Hermet, M. P. Ljungberg, P. Ghosez, and J. Íñiguez, J. Phys. Condens. Matter **25**, 305401 (2013).
[28] I. A. Kornev, L. Bellaiche, P.-E. Janolin, B. Dkhil, and E. Suard, Phys. Rev. Lett. **97**, 157601 (2006).
[29] See Supplemental Material at http://link.aps.org/supplemental/10.1103/PhysRevLett.112.247603, which includes Refs. [17, 18, 27, 31–33, 39–49], for a brief description of various technicalities of our calculations and some complementary results and analysis.
[30] For the FE phase of PTO, our model potential predicts long and short lattice constants of 4.21 Å and 3.94 Å, respectively. In contrast, our PBEsol calculations render 4.03 Å and 3.87 Å for these quantities. These results are consistent with those in Figs. 1(b) and 1(c), as the smaller lattice parameters lead to relatively small polar distortions, both in the domains and within the DWs, in the PBEsol (I) case.
[31] S. Pöykkö and D. J. Chadi, Appl. Phys. Lett. **75**, 2830 (1999).
[32] B. Meyer and D. Vanderbilt, Phys. Rev. B **65**, 104111 (2002).
[33] L. He and D. Vanderbilt, Phys. Rev. B **68**, 134103 (2003).
[34] In this high-T regime, the DW presents all the symmetries that are common to its neighboring domains.
[35] S. K. Streiffer, J. A. Eastman, D. D. Fong, C. Thompson, A. Munkholm, M. V. Ramana Murty, O. Auciello, G. R. Bai, and G. B. Stephenson, Phys. Rev. Lett. **89**, 067601 (2002).
[36] P. Zubko, N. Stucki, C. Lichtensteiger, and J. M. Triscone, Phys. Rev. Lett. **104**, 187601 (2010).
[37] P. Zubko, N. Jecklin, A. Torres-Pardo, P. Aguado-Puente, A. Gloter, C. Lichtensteiger, J. Junquera, O. Stéphan, and J. M. Triscone, Nano Lett. **12**, 2846 (2012).
[38] K. Momma and F. Izumi, J. Appl. Crystallogr. **41**, 653 (2008).
[39] J. P. Perdew, A. Ruzsinszky, G. I. Csonka, O. A. Vydrov, G. E. Scuseria, L. A. Constantin, X. Zhou, and K. Burke, Phys. Rev. Lett. **100**, 136406 (2008).
[40] G. Kresse and J. Furthmüller, Phys. Rev. B **54**, 11169 (1996).
[41] R. Wahl, D. Vogtenhuber, and G. Kresse, Phys. Rev. B **78**, 104116 (2008).
[42] P. E. Blöchl, Phys. Rev. B **50**, 17953 (1994).
[43] G. Kresse and D. Joubert, Phys. Rev. B **59**, 1758 (1999).
[44] W. Zhong, D. Vanderbilt, and K. M. Rabe, Phys. Rev. B **52**, 6301 (1995).
[45] X.-K. Wei, A. K. Tagantsev, A. Kvasov, K. Roleder, C.-L. Jia, and N. Setter, Nat. Commun. **5**, 3031 (2014).
[46] E. Bousquet, M. Dawber, N. Stucki, C. Lichtensteiger, P. Hermet, S. Gariglio, J.-M. Triscone, and P. Ghosez, Nature (London) **452**, 732 (2008).
[47] N. A. Benedek and C. J. Fennie, Phys. Rev. Lett. **106**, 107204 (2011).
[48] Z. Zanolli, J. C. Wojdeł, J. Íñiguez, and P. Ghosez, Phys. Rev. B **88**, 060102 (2013).
[49] Y. Yang, J. Íñiguez, A.-J. Mao, and L. Bellaiche, Phys. Rev. Lett. **112**, 057202 (2014).